ISSN 1061-933X, Colloid Journal, 2017, Vol. 79, No. 1, pp. 1–12. © Pleiades Publishing, Ltd., 2017.
Original Russian Text © G.A. Arshakyan, N.M. Zadymova, 2016, published in Kolloidnyi Zhurnal, 2016, Vol. 78, No. 6, pp. 688–699.

The Effect of a Lipophilic Drug, Felodipine, on the Formation of Nanoemulsions upon Phase Inversion Induced by Temperature Variation

G. A. Arshakyan and N. M. Zadymova*

Department of Chemistry, Moscow State University, Moscow, 119991 Russia
**e-mail: zadymova@colloid.chem.msu.ru*

Received May 30, 2016

Abstract—The correlation between a dispersed phase/dispersion medium interfacial tension σ at a storage temperature of 22°C and the dispersity and stability of oil-in-water miniemulsions, which result from temperature-induced phase inversion, has been revealed for hydrocarbon/polyoxyethylene(4)lauryl ether/water systems (in the presence and absence of felodipine) with the help of conductometry, tensiometry, and dispersion analysis. At $\sigma < 3.5 \times 10^{-6}$ N/m, oil-in-water nanoemulsions, which have narrow monomodal particle size distributions and are stable for a month, are a fortiori formed. Felodipine has been shown to serve as a cosurfactant, which is incorporated into the adsorption layer of a basic stabilizing nonionic surfactant. Therewith, σ values increase and the temperature of phase inversion decreases, while the concentration of the basic surfactant in an optimal composition must be substantially reduced. A heptane/water nanoemulsion (droplet size of 75 nm) stabilized with a basic nonionic surfactant and Tween 80 exhibits a high solubilization capacity with respect to felodipine and ensures its efficient mass transfer through a model membrane.

DOI: 10.1134/S1061933X16060028

1. INTRODUCTION

In recent decades, the development of drug dosage forms that increase the bioavailability and efficiency of already-available drugs has acquired a doubtless practical and scientific significance, because it makes it possible to markedly decrease the duration and expenditure as compared with the elaboration, approbation, and manufacturing application of new drugs. The urgency of the problem is aggravated by the fact that most of the modern drugs are lipophilic and poorly soluble in water, with this circumstance substantially decreasing their bioavailability [1–3]. To increase the bioavailability of lipophilic drugs and protect them from hydrolysis and other types of degradation, including enzymolysis, they may be incorporated into nanosized particles, such as micelles, liposomes, niosomes, vesicles, and droplets of oil-in-water micro- and nanoemulsions, that are capable of transporting them in aqueous media [4–10].

Nanoemulsions represent a specific type of liquid/liquid dispersions, which have average particle radius r_{av} in a range of 10–100 nm and a narrow particle size distribution [11–13]. Sometimes, so-called "miniemulsions" containing dispersed phase particles with submicron sizes (diameter $d < 1$ μm) and average diameter d_{av} lying in a range of 100–500 nm are incorrectly attributed to nanoemulsions [14]. Nanoemulsions are distinguished by kinetic stability, optical transparency (sometimes, they are only slightly opalescent even at a high dispersed phase content), low viscosity, highly developed interfacial surface possessing high adsorption capacity, and ability to penetrate through organs and tissues of the human organism and transport drugs of different natures [10, 15–17]. The unique properties of nanoemulsions are attracting increasing worldwide interest of researchers in them and make them promising for application in pharmacology, cosmetology, veterinary medicine, food industry, etc. All of this especially concerns oil-in-water (O/W) nanoemulsions.

As has been emphasized in a number of reviews [12, 15–18], in contrast to self-organized disperse systems (microemulsions, micellar solutions, and surfactant-based lyotropic liquid crystals), nanoemulsions are thermodynamically unstable, although they can, under certain conditions, retain their properties and particle size distribution unchanged for a long time. Dispersed phases of both nano- and microemulsions are known to be composed of nanosized particles; however, these disperse systems differ fundamentally from each other in accordance with the detailed analysis performed in [19, 20]. In particular, nanoemulsions are advantageous in having a simpler component composition and a much lower surfactant concentration.

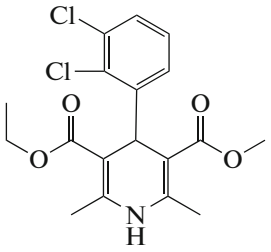

Fig. 1. Structural formula of FD.

Nanoemulsions are most commonly produced by high-energy methods using high-pressure homogenizers, fluidizers, or ultrasonic dispersers [21–25]. These methods are, as a rule, based on empirical optimization of the preparation procedure, nanoemulsion composition, and selection of stabilizing surfactants [26–30]. At the same time, due attention is not always focused on the physicochemical foundations of nanoemulsion stabilization with respect to coalescence, flocculation, and Ostwald ripening (isothermal distillation), which lead to nanoemulsion degradation.

Recently, low-energy nanoemulsion production methods, which entail only slight stirring and are very economical, have drawn increasing attention of researchers [31–36]. These methods are believed to yield stable nanoemulsions with smaller particle sizes than do high-energy methods. Classifications of the low-energy methods are diverse and often misleading. The classification based on the presence or absence of emulsion phase inversion, which is accompanied by a spontaneous change in the curvature of an interfacial surfactant layer, seems to be rather simple and reasonable. According to this classification, a method in which the formation of a nanoemulsion is induced by a rapid transfer of surfactant or dispersed phase molecules to a dispersion medium without a reversal in the sign of the interface curvature is referred to as "self-emulsification." If emulsification is associated with a spontaneous change in the curvature of a stabilizing surfactant layer, which is accompanied by a change in the type of an emulsion, these methods are classified as phase inversion methods. Phase inversion during the formation of nanoemulsions may be initiated by either a change in the composition (Phase Inversion Composition (PIC method), which is sometimes referred to as the EIP (Emulsion Inversion Phase) method) [37–42] or a change in temperature (Phase Inversion Temperature (PIT) method) [35, 36, 43, 44].

The PIT method, which is believed to be most promising for the production of nanoemulsions [35, 36, 45–47], was proposed by Shinoda et al. [43, 44]. This method may be implemented with the use of polyethoxylated nonionic surfactants (NSs), the solubility of which strongly depends on temperature. In this case, the PIT, which is sometimes referred to as the "hydrophilic–lipophilic balance temperature" (T_{HLB}), is the key physicochemical parameter. This temperature corresponds to the coincidence between the solubilities of a stabilizing NS in water and oil, which leads to the zero curvature of the interfacial layer and ultralow values of the interfacial tension [36, 43, 44]. At a temperature below PIT, when polyethoxylated chains are hydrated and a stabilizing NS has higher affinity for water than for oil, an O/W emulsion is formed. When the temperature is higher than PIT, the NS is dehydrated, it becomes lipophilic and stabilizes water-in-oil (W/O) emulsions. The PIT method consists in careful dispersing of an emulsion at T_{HLB} followed by rapid cooling or heating for the formation of O/W or W/O nanoemulsions, respectively [43, 44].

It should, however, be noted that the PIT method, i.e., the temperature-variation-induced phase inversion, does not always ensure the formation of stable nanoemulsions [48, 49]. The reasons for this and the mechanisms of nanoemulsion formation still remain hypothetical and debatable. At the same time, nanoemulsions are, as a rule, stabilized using a rather narrow spectrum of NSs or their mixtures, which are not always suitable for medical application. In most cases, nanoemulsions obtained by the PIT method contain additives of electrolytes (commonly, NaCl), because of the necessity to determine the PIT value by the electrical conductivity method; however, this is often undesirable from the medical point of view. There is so far actually no information on the effect of lipophilic drugs on the PIT values, properties, and stability of nanoemulsions. We have found only two works devoted to the influence of ibuprofen [50] and α-tocopherol [51] on the PIT values and dispersity of O/W nanoemulsions.

The goal of this work was to study the effect of a lipophilic drug, felodipine, on the PIT in heptane/polyoxyethylene(4)lauryl ether/water systems and the dispersity and stability of nanoemulsions obtained by the PIT method with the aim of efficient incorporation of the drug into O/W nanoemulsions.

2. EXPERIMENTAL

2.1. Objects

Felodipine base (FD, (*RS*)-3-ethyl-5-methyl-4-(2,3-dichlorophenyl)-2,6-dimethyl-1,4-dihydropyridine-3,5-dicarboxylate) is a modern antihypertensive and antianginal drug, calcium channel blocker [52]. The structural formula of FD is presented in Fig. 1. This lipophilic drug has a very low solubility in water ($S_w = 2.2 \times 10^{-6}$ M [6]) and a low bioavailability of no higher than 20% upon oral administration. FD is electrically neutral, stable in solutions, and almost unaffected by pH; its molecular weight is $M_w = 384.2$ Da.

The aforementioned characteristics make FD a good model drug for the development of colloidochemical foundations for the production of stable

O/W nanoemulsions containing incorporated drugs. FD produced by PCAS Co. (Finland) with a purity of 99% was used in the work.

Polyoxyethylene(4)lauryl ether (Brij® L4, BR), which is rather frequently used for the preparation of nanoemulsions by the PIT method [36, 45, 53], was chosen as a basic stabilizer. This NS is not micelle-forming and is poorly soluble in aqueous media; according to the data of the manufacturer (Sigma-Aldrich, United States), its HLB = 9.7, and $M_w \approx$ 362 Da [54].

A hydrophilic micelle-forming NS, polyoxyethylene(20)sorbitan monooleate (Tween® 80, Tw) with HLB = 15 [55], $M_w \approx$ 1310 Da, and critical micelle concentration (CMC) of 0.012 mM [54] (Sigma-Aldrich), was sometimes used as an additional stabilizer as received.

The NSs used in the work had been approved by the United States Food and Drug Administration to be used in the medicine and food industries.

Heptane and decane, which have greatly different solubilities in water, were selected as dispersed phases of emulsions to study the effect of the Ostwald ripening on their stability.

Organic solvents (heptane, decane, ethanol, and *n*-propanol, Sigma-Aldrich) were of reagent grade.

Triply distilled water with electrical conductivity κ equal to 1.5 μS/cm (22°C) was used in the experiments. In all cases, sodium azide (0.01 wt %, i.e., in a concentration 66–3300 times lower than NaCl concentrations used upon conductometric determination of PIT values [56, 57]) was added to water to prevent the components of the emulsions from bacterial degradation. The κ value of the aqueous sodium azide solutions was 187 μS/cm (22°C).

2.2. Methods

2.2.1. Conductometric Examination of Emulsions at Different Temperatures

Electrical conductivity of emulsions was measured at different temperatures (10–95°C) using a setup composed of an LC 120 universal shaker (LAB-PU-02, Russia), a thermostated sealed glass cell with an inlet for a temperature controller probe, a FiveGo™ FG3 conductometer (Mettler-Toledo, Switzerland), and a water circulation thermostat. The oscillation frequency and amplitude of the back-and-forth motion of the shaker platform were 250 min^{-1} and 10 mm, respectively. Specific conductivity was measured while varying temperature with steps of 0.1°C at an accuracy of ±0.5%. Emulsion sample volumes were in a range of 30–33 cm^3. The heating rate was 1°C/min.

The $\kappa(T)$ curves for the temperature dependences of specific conductivity were employed to determine the PIT values for different emulsion compositions. The PIT values were determined as means of temperature values corresponding to the maximum and minimum (i.e., equal to zero) specific conductivities of the emulsions [43, 44]. In addition, the PIT values were found as temperatures corresponding to the minimum in the dependence of $d\kappa/dT$ derivative on T.

2.2.2. UV Spectroscopy

FD solubility in heptane BR solutions was found spectrophotometrically with an Agilent 8453 single-beam spectrophotometer (United States) operating in a wavelength range of 200–1000 nm. The spectra were measured relative to solutions with the same compositions, but free of the drug. Quartz cells with a thickness of 1 cm were used for the measurements. Absorbance A was determined with an accuracy of $\pm 1 \times 10^{-4}$ rel. units.

Heptane BR solutions with different concentrations were preliminarily saturated with FD. For this purpose, excess amounts of the drug were added to them, and the mixtures were stored in dark under periodic stirring on a magnetic stirrer until equilibrium solubility values were reached in accordance with spectrophotometric data. Before the spectrophotometric measurements, a sample of a supernatant over an FD sediment was carefully taken and filtered (0.22 μm, Millipore); then, the sample was diluted with *n*-propanol, in which the FD absorption maximum was, according to our data, observed at wavelength $\lambda_{max} = 363$ nm, while the value of molar extinction coefficient E_{max} corresponding to the absorption maximum was 6795 ± 20 M^{-1} cm^{-1} (22°C). The values of FD solubility S_F were calculated by the following relation:

$$S_F = (A_{max}/E_{max})P,$$

where A_{max} is the absorbance of an examined diluted sample at $\lambda_{max} = 363$ nm and P is the dilution of the sample, which was equal to 101–301 times.

2.2.3. Precise Turbidimetry

Solubility of BR in an aqueous sodium azide solution was studied by a precise turbidimetry procedure, which we had developed earlier [58]. The efficiency of this procedure was confirmed for the determination of the solubility of lipophilic NSs with low HLB values and perfluorodecalin in water and aqueous micellar solutions of hydrophilic NSs [5, 6, 58, 59].

An accurately weighed portion of BR was dispersed in an aqueous sodium azide solution using a UZDN ultrasonic disperser (Russia) operating at a frequency of 22 kHz with subsequent cooling for 1 min. A series of extremely diluted emulsions with known molar BR concentrations ($C_{BR} = (0.86–5.02) \times 10^{-4}$ M) was prepared by diluting the obtained emulsion with the aqueous sodium azide solution. The resulting emulsions were stable to aggregation and sedimentation for

a long time; their spectra were recorded with an Agilent 8453 spectrophotometer (see Section *2.2.2*) in a wide wavelength range (200–1000 nm) at preset time intervals t after the moment of preparation. These data were employed to determine the equilibrium solubility of the studied lipophilic NS in the aqueous sodium azide solution ($S_{BR} = 9.1 \times 10^{-4}$ M, 22°C) by the procedure that we had previously described in detail elsewhere [5, 6, 58, 59].

2.2.4. Tensiometry at Different Temperatures

Interfacial tension σ was measured by the rotating droplet method with a SITE 100 tensiometer (Krüss, Germany), operating in the range of ultralow σ values (lower than 10^{-6} mN/m) and a wide temperature range (from 0 to 100°C). The rotation rate of a capillary tube 2.5 mm in diameter filled with an examined aqueous phase was varied from 2000 to 6000 rpm, while the volume of a nonpolar liquid droplet introduced into the tube was 0.2–1 μL. Being rotated in an optimum regime, the droplet of the nonpolar liquid (an NS solution in heptane) acquired a cylindrical shape. The volume of an introduced droplet and the rotation rate of the capillary tube were chosen in a manner such that the length of the nonpolar liquid cylinder was four times larger than its diameter. The interfacial tension was calculated using the DSA2 software (Krüss) directly in the course of the experiment by the following relation:

$$\sigma = k\omega^2 r^3(\rho_w - \rho_o),$$

where k is an instrument constant, which depends on the optics magnification factor (3× or 5×); ω is the angular rotation rate of the capillary tube about its major axis; r is the radius of the rotating cylindrical droplet; and ρ_w and ρ_o are the densities of the aqueous and oil phases ($\rho_w > \rho_o$), respectively, which were determined by pycnometry with an accuracy of ± 0.0005 g/cm^3 in advance.

The σ values of BR solutions in a hydrocarbon (in the presence and absence of the drug) at the boundary with the sodium azide solution were begun to be measured at a temperature above PIT; then, it was gradually decreased. Readings were recorded every 2–5°C after thorough thermostating. In a temperature range of $T <$ PIT, a sodium azide solution with BR concentration equal to its equilibrium solubility (Section *2.2.3*) was used as an aqueous phase to avoid intense transfer of the NS from the nonpolar phase to water, which is accompanied by blurring of the droplet contour and makes the calculation of the interfacial tension impossible. The measurements were performed while increasing the temperature. This enabled us to avoid the problems that the authors of [60] encountered when unsuccessfully trying to measure the interfacial tension by the rotating droplet method at the paraffin oil/water interface in the presence of mixed HSs (Tw + Span 80 or Brij 96 + Brij 92).

2.2.5. Preparation of Nanoemulsions

O/W nanoemulsions were prepared by the PIT method [43, 44] taking into account the corresponding temperature values that we had determined for the emulsion compositions being elaborated. The compositions were prepared from BR solutions in hydrocarbons (heptane or decane) with different concentrations ($C_{BR} = 6.7$–16.6 wt %) and the aqueous sodium azide solution. Hydrocarbon content was, in all cases, 20 wt %. A prepared mixture was placed into a sealed glass vessel and dispersed for 20 min on a magnetic stirrer (1200 rpm) at room temperature. Then, the mixture was exposed for 30 min at PIT in a thermostated chamber (Binder, Germany) under conditions of forced air circulation and continuous stirring. After that, the emulsion was abruptly cooled on an ice bath and stored at room temperature ($T_{st} = 22 \pm 1$°C) with periodic control over particle sizes.

When FD was incorporated into the nanoemulsions, an analogous procedure was employed with the only difference that the used BR solutions in heptane were preliminarily saturated with FD. In a number of cases, the aqueous phase contained Tw.

2.2.6. Dispersion Analysis

Particle size distribution in the emulsions was studied by dynamic light scattering with a Zetatrac™ high-speed analyzer (NPA152 model, Microtrac Inc., United States) operating in the mode of laser diffraction. A laser diode served as a source of radiation with a wavelength of 730 nm. An aqueous 0.01 wt % sodium azide solution, which was used as the dispersion medium of the emulsions, served as a reference medium. For each sample, periodic measurements were performed for 60–120 min with intervals of 3–6 min. The time was counted from the moment of emulsion preparation. The data obtained were processed using the Microtrac FLEX Software. Differential distribution curves characterizing the volume fraction (or volume percentage) of particles of each diameter were obtained.

2.2.7. Determination of Felodipine Mass Transfer

The rate of FD mass transfer by dispersed phase particles of O/W nanoemulsions was measured in a Franz-type diffusion cell consisting of donor and acceptor chambers separated with a membrane. MF-Millipore membranes made of a biologically inert mixture of cellulose esters (pore diameter, thickness, and porosity of 0.45 μm, 150 μm, and 75%, respectively) were used. Such membranes are employed to analyze the rate of drug release from microemulsions [61]. A magnetic stirrer and a receptor medium possessing a high dissolving ability with respect to the desired component were placed into the acceptor chamber of the Franz-type cell. A water/ethanol

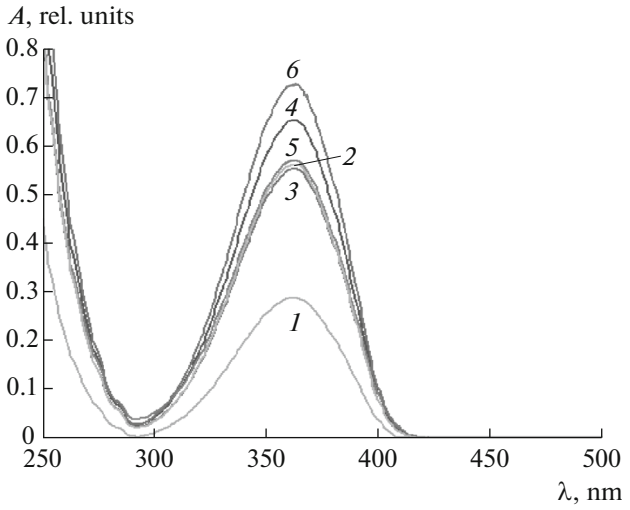

Fig. 2. FD absorption spectra used for determining its solubility in heptane BR solutions with different concentrations (wt %): (*1*) 2.0 (by 109 times), (*2*) 5.8 (109), (*3*) 6.7 (136), (*4*) 8.0 (136), (*5*) 11.9 (271), and (*6*) 16.6 (301). Parenthetic numerals represent the degrees of saturated FD solution sample dilution with *n*-propanol.

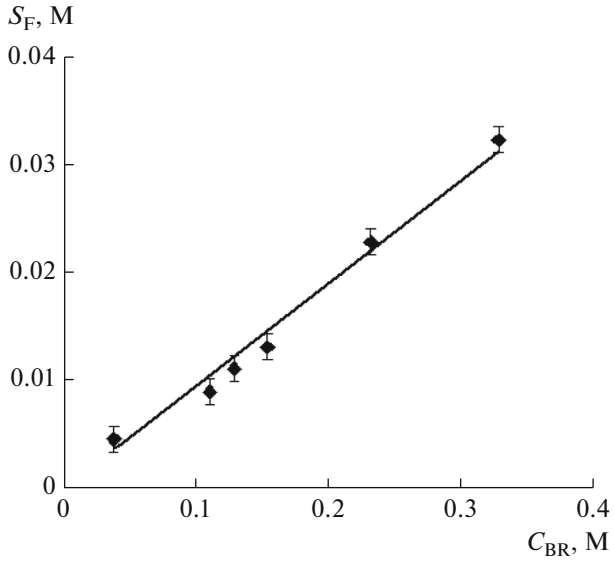

Fig. 3. Equilibrium isotherm of felodipine solubilization in heptane BR solutions with different concentrations at 22°C.

binary mixture (60/40, weight/weight) has been recommended as the receptor medium for FD [62].

Felodipine amount I_F that had diffused through unit area over time t was calculated by the following equation:

$$I_F = C_F V/a_0,$$

where V is the receptor medium volume (7.5 cm^3); a_0 is the area through which the drug diffuses, this area being equal to the membrane-covered orifice in the Fanz-type cell (0.71 cm^2); and C_F is the FD concentration in the receptor medium at time moment t, this concentration being determined by UV spectroscopy using the extinction coefficient, which we found for FD in the receptor medium ($E_{364} = 6943 \pm 20$ M^{-1} cm^{-1} at 22°C). Samples were taken at preset time intervals; the undiluted samples were analyzed and returned into the diffusion cell.

The experiments were repeated five or six times, and average I_F values were calculated. The time dependences of I_F were used to determine the rate of the diffusion mass transfer of the desired component.

3. RESULTS AND DISCUSSION

The PIT values of hydrocarbon/BR/aqueous sodium azide solution emulsion compositions were determined by conductometry in the absence and presence of FD. BR concentration C_{BR} in a hydrocarbon was varied in a range of 2.0–16.6 wt %. The mass fraction of a hydrocarbon in emulsions was equal to 0.2.

To incorporate the drug into the emulsions, BR solutions in hydrocarbons were saturated with FD, the concentration of which was determined by UV spectroscopy (Section *2.2.2*). Figure 2 exemplifies the absorption spectra that were used to estimate FD solubility S_F in heptane BR solutions. The FD solubility linearly increases with BR concentration (Fig. 3) seemingly due to the solubilization of the studied lipophilic drug in reverse BR micelles. The slope of the $S_F(C_{BR})$ solubilization isotherm (Fig. 3) characterizes the solubilization capacity (SC) of reverse BR micelles with respect to FD (SC = 0.095 mol/mol), i.e., the ratio between the numbers of molecules (or moles) of the solubilisate and solubilizer in micelles. It should be emphasized that the solubility of FD in a 16.6 wt % BR solution is nearly 60 times higher than its solubility in heptane. Thus, the concentration of the drug in nanoemulsions may be controlled by varying BR concentration in the hydrocarbon.

The PIT values were determined from the temperature dependences of specific conductivity κ and its derivative $d\kappa/dT$. The most typical results are shown in Figs. 4–6. The following regularities have been revealed for the studied emulsion systems.

1. A rise in hydrocarbon molecular mass causes an increase in PIT at the same component composition (Fig. 4).

2. The PIT value substantially decreases with a growth in the concentration of a stabilizing surfactant in the hydrocarbon (Fig. 5).

3. The introduction of a hydrophilic NS is accompanied by an increase in PIT (Fig. 6).

4. FD induces a substantial decrease in PIT at the same component composition (Fig. 7).

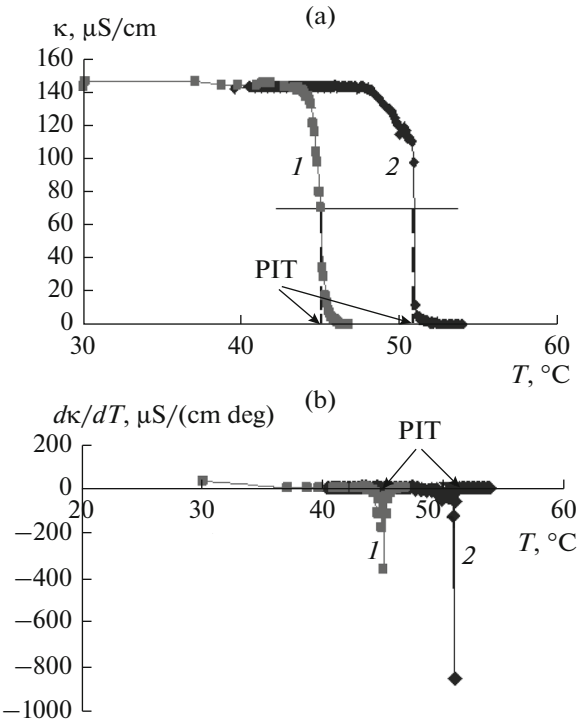

Fig. 4. Temperature dependences of (a) specific conductivity and (b) its temperature derivative for hydrocarbon/BR/aqueous sodium azide solution systems: (*1*) heptane and (*2*) decane. BR concentration in a hydrocarbon is 8 wt %.

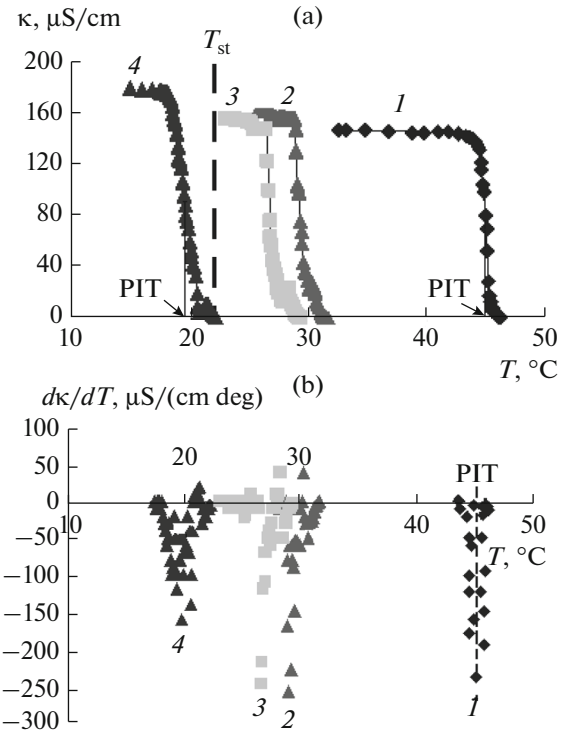

Fig. 5. Determination of PIT from the temperature dependences of (a) specific conductivity and (b) its temperature derivative for heptane/BR/aqueous sodium azide solution emulsions at different stabilizer concentrations: (*1*) 8.0, (*2*) 11.9, (*3*) 12.8, and (*4*) 16.6 wt %.

The PIT values served as the basis for the preparation of O/W miniemulsions by the method of temperature-induced phase inversion. We have obtained 30 emulsions; however, only those with PIT > T_{st} appeared to be O/W emulsions at room temperature. When PIT < T_{st}, W/O emulsions are formed at T_{st} = 22°C (Fig. 7), which are outside of the scope of this communication.

Since we further intend to incorporate O/W nanoemulsions into solutions of polymer adhesives with the purpose of developing polymer matrixes for drug delivery, with strict requirements being imposed on these matrices concerning the limitation of the residual content of organic solvents, the main results were obtained for emulsions based on heptane, which is more volatile than decane is.

Dispersion analysis was performed for O/W emulsions obtained by the PIT method and stored for different time periods (from 0.1 h to 30 days). It has been shown that the concentration of the basic stabilizing NS substantially affects their dispersity and stability. As C_{BR} is increased, O/W emulsions containing submicron particles growing with time and having a wide size distribution (Fig. 8a) transform into emulsions having a bimodal distribution and containing fraction of nanosized droplets (Fig. 8b) and, further, to stable nanoemulsions with a narrow particle size distribution (Fig. 8c).

To answer the question as to the identity of the reasons for the different results of the PIT method, precise measurements of interfacial tension σ were per-

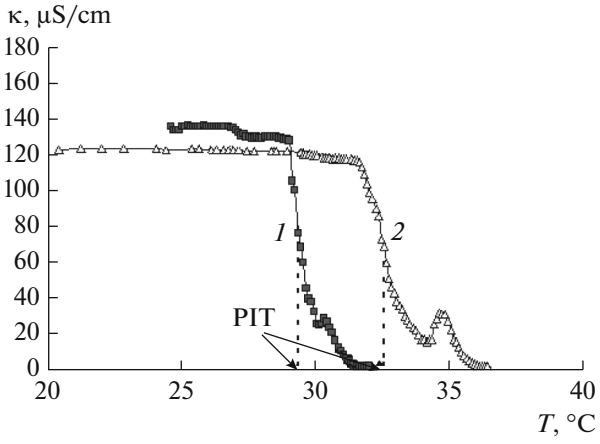

Fig. 6. Temperature dependences of specific conductivity for heptane/BR/aqueous sodium azide solution systems in the (*1*) absence and (*2*) presence of Tw. Concentrations of BR in heptane and Tw in water are 11.9 and 0.9 wt %, respectively.

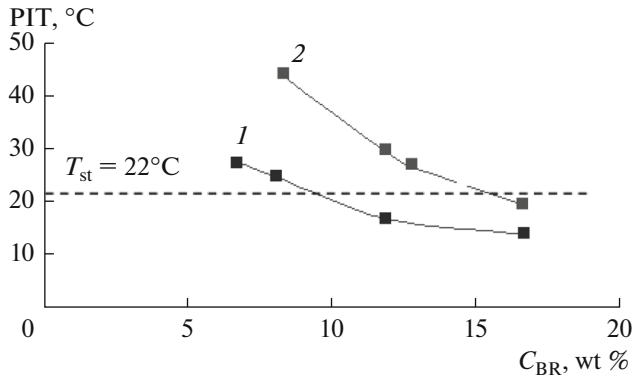

Fig. 7. Dependences of PIT values on NS concentration in heptane solutions for heptane/BR/aqueous sodium azide solution systems in the (*1*) presence and (*2*) absence of FD.

formed for BR solutions in heptane at a boundary with an aqueous sodium azide solution at different temperatures in the absence and presence of FD (Fig. 9) and for a 8 wt % BR solution in decane (Fig. 10). The minima in the $\sigma(T)$ dependences corresponded to the PIT values of the studied emulsion systems and were in good agreement with the conductometry data (Fig. 7). These dependences were also used to determine the values of the interfacial tension at T_{HLB} and T_{st}.

The comparison between the tensiometry and dispersion analysis data has shown a reliable correlation between the values of interfacial tension at PIT and T_{st} and the properties of the obtained emulsions (see Table 1). It is obvious that the lower the interfacial tension at the temperature of HLB the more intense the dispersion process, which is initiated by the intense NS mass transfer to the aqueous phase upon rapid cooling. In this case, smaller particles of dispersed oil phase will be formed. Moreover, the lower σ at the interface in an emulsion at T_{st}, the less intense the processes of emulsion degradation via coagulation, coalescence, and Ostwald ripening and the more stable an obtained O/W emulsion will be.

It should be especially emphasized that the results of our tensiometric measurements are in good agreement with the data of frequently-cited work [63] (see, e.g., [64, 65]), in which interfacial tension σ_{ab} has been measured for microemulsions, which belong to types I, II, and III according to Winsor's classification and are based on water/*n*-alkan/alkyl polyglycoesters of different structures systems. For type-I microemulsions, σ_{ab} corresponds to the interface between an O/W microemulsion and an excess oil phase occurring at equilibrium with it. For type-II microemulsions, it corresponds to the interface between a W/O microemulsion and an equilibrium excess aqueous phase. For type-III microemulsions, it characterizes the interface between equilibrium excess aqueous and oil phases (with a bicontinuous microemulsion located between them), the necessary amounts of which have been taken from a three-phase system and artificially brought into contact in a Spinning drop tensiometer [63]. As the temperature is elevated, the I → III → II structural transformations occur in the microemul-

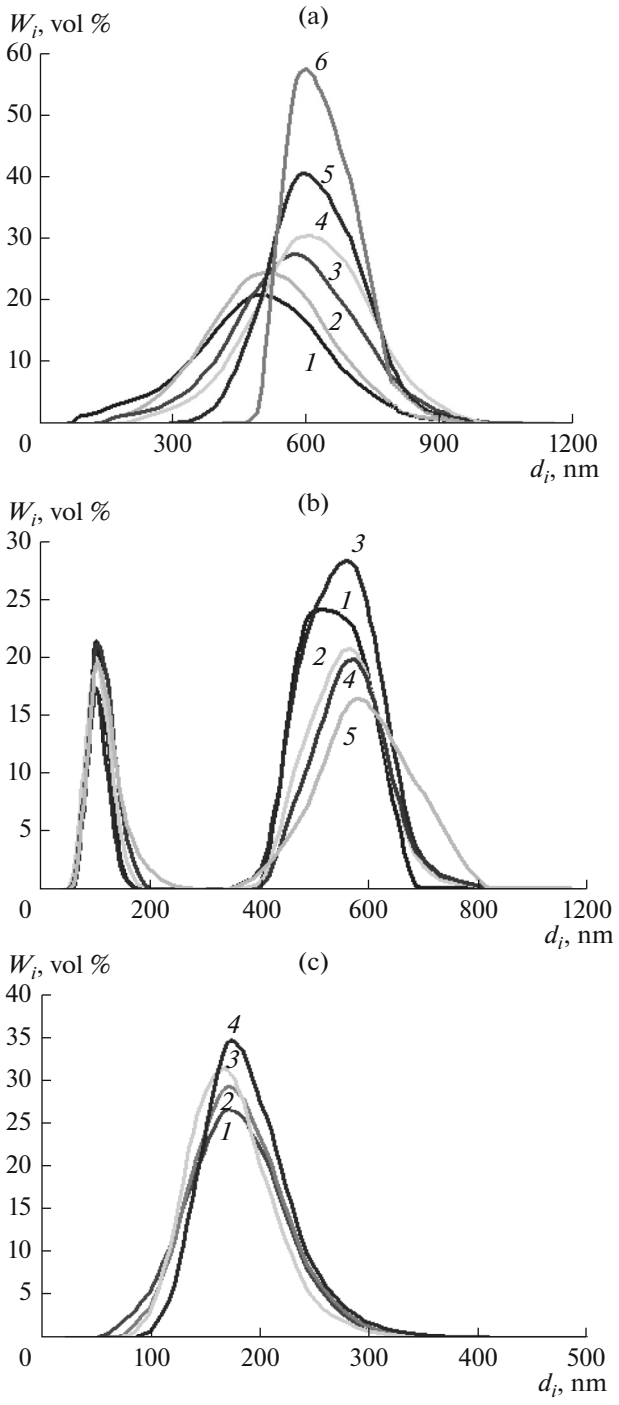

Fig. 8. Differential curves of dispersed phase particle size distribution for heptane/water emulsions obtained at BR concentrations of (a) 8.0, (b) 11.9, and (c) 12.8 wt % and different durations of storage at 22°C: (a) (*1*) 0.1, (*2*) 3, (*3*) 4.5, (*4*) 22, and (*5*) 120 h; (b) (*1*) 25, (*2*) 45, (*3*) 69, and (*4*) 117–496 h; and (c) (*1*) 18, (*2*) 69, (*3*) 140, and (*4*) 720 h.

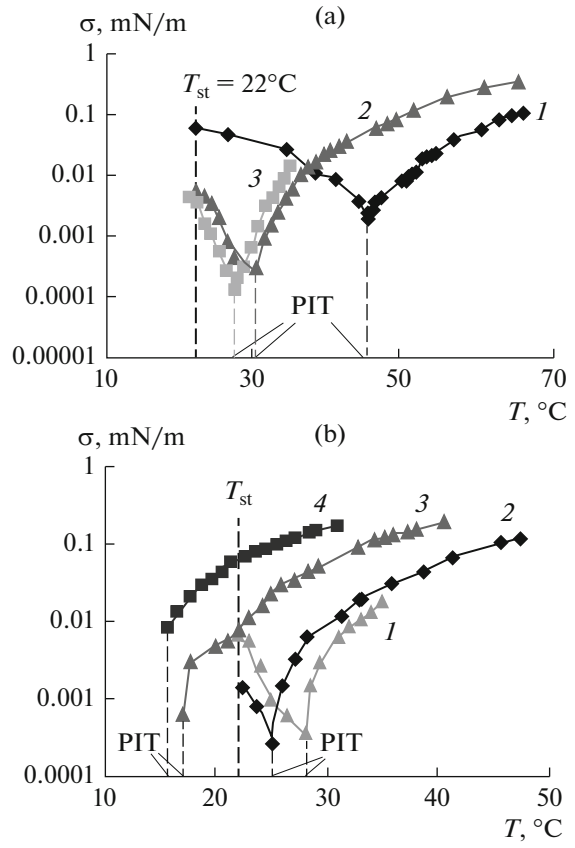

Fig. 9. Temperature dependences of interfacial tension at heptane BR solution/aqueous sodium azide solution interfaces at different NS concentrations in the (a) absence and (b) presence of FD: (a) (*1*) 8.0, (*2*) 11.9, and (*3*) 12.8 wt % and (b) (*1*) 6.7, (*2*) 8.0, (*3*) 11.9, and (*4*) 16.6 wt %. BR solutions in heptane are saturated with FD.

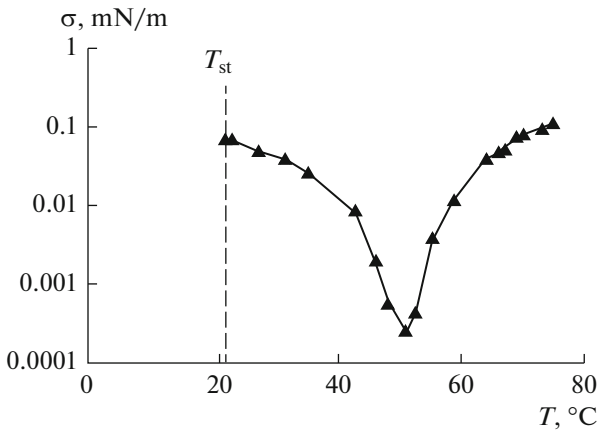

Fig. 10. Temperature dependence of interfacial tension for 8 wt % BR solution in decane at an interface with an aqueous sodium azide solution.

sions, and the temperature dependence of σ_{ab} exhibits a minimum (~10^{-5} N/m) corresponding to a microemulsion with a bicontinuous structure [63]. Since the polytherms of interfacial tension (Figs. 9, 10) are similar to the $\sigma_{ab}(T)$ dependences [63], and the values of σ at PIT correspond to the minimum and amount to ~10^{-6}–10^{-7} N/m (see Table 1), it may be assumed that bicontinuous microemulsions are formed in the examined systems at PIT.

The tensiometry data were taken into account when analyzing the effect of Ostwald ripening (OR) on the dispersity and stability of emulsions using the Lifshitz–Slyozov–Wagner (LSW) equation, according to which, the rate of OR under quasi-stationary conditions is constant and determined as follows [66–68]:

$$\omega = dr_c^3/dt = 8\sigma DC_\infty V_m/9RT \cong dr_{av}^3/dt,$$

where r_c is the critical radius characterizing particles that, at a given time moment, are in unstable equilibrium with a dispersion medium, with the sizes of particles having $r < r_c$ decreasing, while the sizes of particles with $r > r_c$ are increasing; r_{av} is the average particle radius that approximates r_c [69, 70]; D is the diffusion coefficient of dispersed phase molecules in a dispersion medium; and concentration C_∞ is expressed as volume fraction [69, 70].

At C_{BR} = 8 wt %, when the values of the interfacial tension for both studied hydrocarbons at T_{st} are rather close to each other (Table 1), polydisperse emulsions are formed with submicron particle sizes (Fig. 8a). Figure 11 shows the $r_{av}^3(t)$ dependences for such emulsions. The maximum rates of droplet growth of 383 and 19 nm^3/s for heptane- and decane-based miniemulsions, respectively, were determined from the initial linear parts of these dependences. The higher degradation rate for miniemulations with hydrocarbon more soluble in water confirms the substantial effect of OR. However, the $r_{av}^3(t)$ dependences are nonlinear and cannot be described by the LSW equation (Fig. 11). The parameters of this equation used in the calculations, as well as the calculated values of OR rate (ω_{LSW}), are presented in Table 2. The data obtained have shown that the particles grow due to OR and coalescence.

When the interfacial tension at T_{st} decreases to ≈6 × 10^{-6} N/m, the PIT method yields emulsions that have a bimodal particle size distribution with a substantial fraction of nanosized particles (Table 1, Fig. 8b). At σ values of ~10^{-7} and 10^{-6} N/m at PIT and T_{st}, respectively, this approach ensures the formation of stable O/W nanoemulsions with a narrow particle size distribution (Table 1, Fig. 8c).

Thus, the temperature dependences of the interfacial tension at the dispersed phase/dispersion medium model interfaces plotted for the range comprising PIT and T_{st} make it possible to predict the perspectives for

Table 1. The values of PIT and interfacial tension at a dispersed phase/dispersion medium boundary at PIT and T_{st}, the type of emulsions resulting from phase inversion in hydrocarbon/BR/aqueous sodium azide solution systems with different concentrations of the stabilizer in the presence and absence of incorporated felodipine

C_{BR}, wt %	PIT, °C	PIT – T_{st}, °C	σ_{PIT}, N/m	$\sigma_{T_{st}}$, N/m	Type of emulsion at T_{st} = 22°C
without felodipine					
with *n*-decane					
8.0	50.9	28.9	1.8×10^{-6}	7.4×10^{-5}	O/W monomodal polydisperse
with *n*-heptane					
8.0	45.0	23.0	2.0×10^{-6}	6.0×10^{-5}	O/W monomodal polydisperse
11.9	29.3	7.6	3.0×10^{-7}	5.5×10^{-6}	O/W bimodal with a nanodisperse fraction
12.8	26.7	4.7	1.4×10^{-7}	3.5×10^{-6}	O/W nanoemulsion, $d_{av} \approx 150$ nm
16.6	20.0	–2.0	–	–	W/O
with felodipine					
with *n*-heptane					
6.7	28.1	6.1	6.4×10^{-7}	5.7×10^{-6}	O/W bimodal with a nanodisperse fraction
8.0	25.1	3.1	4.0×10^{-7}	2.3×10^{-6}	O/W nanoemulsion, $d_{av} \approx 150$ nm
11.9	17.1	–4.9	–	–	W/O
12.8	16.5	–5.5	–	–	W/O
16.6	15.9	–6.1	–	–	W/O

the preparation of stable O/W nanoemulsions by the PIT method.

It has been established (Figs. 7, 9) that FD decreases PIT and noticeably reduces (from 12.8 to 8 wt %) the basic stabilizing NS concentration optimum for the formation of O/W nanoemulsions; i.e., it acts as a cosurfactant, which is incorporated into the adsorption layer of the basic NS and hydrophobizes it. This limits the feasibility of elevating FD concentration in O/W nanoemulsions by increasing C_{BR} (see Fig. 3), because, at concentrations higher than 9.5 wt %, the PIT values appear to be lower than room temperature, thus corresponding to the formation of W/O emulsions (Fig. 7).

The incorporation of a hydrophilic surface-active additive (Tw, 0.9 wt %) has made it possible to reach an optimum PIT value (26.7°C) at a higher BR concentration (11.9 wt %) and, accordingly, a higher content of FD in a nanoemulsion (6.25×10^{-3} M, which is 2840 times higher than that in water). The developed O/W nanoemulsion (r_{av} = 75 nm) with a narrow particle size distribution appears to be stable for a month or longer. It ensures a much more efficient FD mass transfer through a model membrane than a micellar

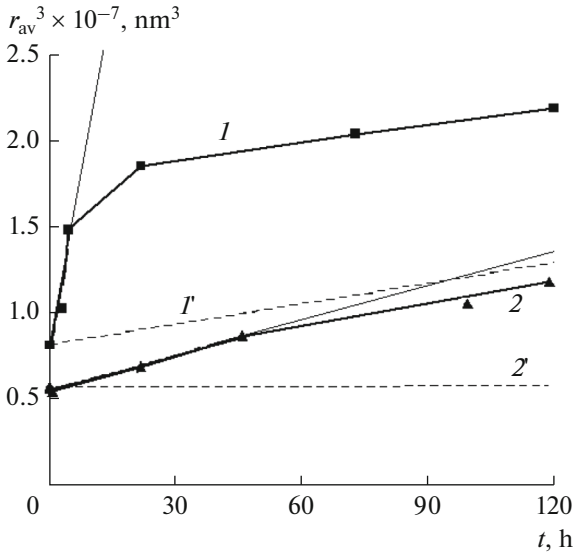

Fig. 11. Time dependences of cubed average particle radii for submicron hydrocarbon/water emulsions stabilized with BR (8 wt %): (*1, 1'*) heptane, (*2, 2'*) decane, (*1*, *2*) experimental data, and (*1'*, *2'*) data calculated by the LSW equation.

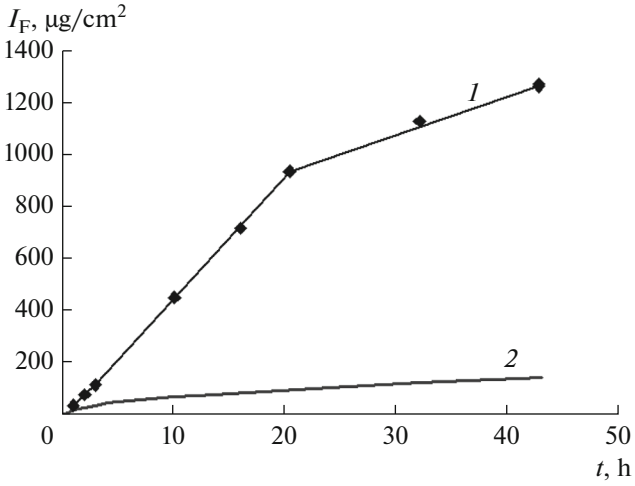

Fig. 12. Time dependences of felodipine mass transfer by (*1*) droplets of the heptane/water nanoemulsion stabilized with BR (11.9 wt %) and Tw and (*2*) Tw micelles [3]. In both cases, Tw concentration in the aqueous phase is 0.915 wt %.

solution of Tw with a corresponding concentration does (Fig. 12).

4. CONCLUSIONS

The effect of lipophilic drugs on the interfacial tension at an oil + NS/water interface, which simulates interfaces of corresponding emulsions, in the vicinity of PIT has not been studied previously. However, the stability and dispersity of emulsions obtained by the method of temperature-induced phase inversion depend namely on the interfacial tension at the dispersed phase/dispersion medium interface.

For hydrocarbon/BR/aqueous sodium azide solution systems (in the presence and absence of FD additives), conductometry, tensiometry, and dispersion analysis data have revealed a correlation between the values of the interfacial tension at a dispersed phase/dispersion medium interface at PIT and T_{st} (22°C) and the dispersity and stability of O/W emulsions. For example, nanoemulsions (average droplet radius $r_{av} < 85$ nm) with a narrow monomodal particle size distribution (stable for a month) are certainly formed when the interfacial tension at PIT is in a range of (1.4–4.0) × 10^{-7} N/m, while, at T_{st}, it is no higher than 3.5 × 10^{-6} N/m.

Thus, it has been proven that the analysis of the temperature dependences of the interfacial tension at hydrocarbon NS solution/water interfaces simulating interfaces in emulsions is efficient from the point of view of predicting an optimum composition for obtaining stable O/W nanoemulsions by the PIT method.

It has been established that FD plays the role of a cosurfactant, which is incorporated into an adsorption layer of a basic stabilizing NS to increase the interfacial tension at a dispersed phase/dispersion medium interface and decrease the PIT value. Therewith, the concentration of the basic HS in a composition optimum for the formation of O/W nanoemulations must be rather low.

Table 2. The values of the parameters entering into the Lifshitz–Slyozov–Wagner equation and the rate of OR (ω_{LSW}) for hydrocarbon/water miniemulsions stabilized with BR (8 wt %)

Parameter*	*n*-Heptane	*n*-Decane
D, m^2/s	7 × 10^{-10} [71]	5.9 × 10^{-10}
V_m, m^3/mol (22°C)	1.47 × 10^{-4}	1.95 × 10^{-4}
C_∞, volume fraction	5.0 × 10^{-6} [72]	7.0 × 10^{-8}
ω_{LSW}, nm^3/s	11.0	0.2

*The values of σ are presented in Table 1.

The PIT method has been employed to obtain a stable heptane/water nanoemulsion (r_{av} = 75 nm) stabilized with BR and Tw; the nanoemulsion has a high solubilization capacity with respect to FD and provides efficient transfer of this drug through a model membrane.

ACKNOWLEDGMENTS

This work was supported by the Russian Foundation for Basic Research, project no. 15-08-04546a.

REFERENCES

1. Lipinski, A., *Am. Pharm. Res.*, 2002, vol. 19, p. 1894.
2. Vemula, V.R., Lagishetty, V., and Lingala, S., *Int. J. Pharm. Sci. Rev. Res.*, 2010, vol. 5, p. 41.
3. Savjani, K.T., Gajjar, A.K., and Savjani, J.K., *SRN Pharm.*, 2012, p. 5402.
4. Rangel-Yagui, C.O., Junior, A.P., and Tavares, L.C., *J. Pharm. Pharm. Sci.*, 2005, vol. 8, no. 2, p. 147.
5. Zadymova, N.M. and Ivanova, N.I., *Colloid J.*, 2013, vol. 75, p. 159.
6. Zadymova, N.M. and Ivanova, N.I., *Moscow Univ. Chem. Bull.*, 2013, vol. 68, p. 112.
7. Malmsten, M., *Surfactants and Polymers in Drug Delivery*, New York: Marcel Dekker, 2002.
8. Malmsten, M., *Soft Matter*, 2006, vol. 2, p. 760.
9. Lawrence, M.J. and Rees, G.D., *Adv. Drug Delivery Rev.*, 2000, vol. 45, p. 89.
10. Lovelyn, C. and Attama, A.A., *J. Biomater. Nanobiotechnol.*, 2011, vol. 2, p. 626.
11. Saha, S. and Ramesh, R., *Int. J. Pharm. Tech. Res.*, 2014–2015, vol. 7, p. 616.
12. Mason, T.G., Wilking, J.N., Meleson, K., Chang, C.B., and Graves, S.M., *J. Phys.: Condens. Matter*, 2006, vol. 18, p. R635.
13. Solans, C., Izquierdo, P., Nolla, J., Azemar, N., and Garcia-Celma, M.J., *Curr. Opin. Colloid Interface Sci.*, 2005, vol. 10, p. 102.
14. Tadros, T., Izquierdo, P., Esquena, J., and Solans, C., *Adv. Colloid Interface Sci.*, 2004, vols. 108–109, p. 303.
15. Fryd, M.M. and Mason, T.G., *Annu. Rev. Phys. Chem.*, 2012, vol. 63, p. 493.
16. Koroleva, M.Yu. and Yurtov, E.V., *Usp. Khim.*, 2012, vol. 81, p. 21.
17. Gupta, A., Eral, H.B., Hattona, T.A., and Doyle, P.S., *Soft Matter*, 2016, vol. 12, p. 2826.
18. Gutierrez, J.M., Gonzalez, C., Maestro, A., Sole, I., Pey, C.M., and Nolla, J., *Curr. Opin. Colloid Interface Sci.*, 2008, vol. 13, p. 245.
19. McClements, D.J., *Soft Matter*, 2012, vol. 8, p. 1719.
20. Anton, N. and Vandamme, T.F., *Pharm. Res.*, 2011, vol. 28, p. 978.
21. Mason, T.G., Graves, S.M., Wilking, J.N., and Lin, M.Y., *Condens. Matter Phys.*, 2006, vol. 9, p. 193.
22. Jafari, S.M., He, Y., and Bhandari, B., *Eur. Food Res. Technol.*, 2007, vol. 225, p. 733.
23. Quin, C. and McClements, D.J., *Food Hydrocolloids*, 2011, vol. 25, p. 1000.
24. Kentish, S., Wooster, T.J., Ashokkumar, M., Balachandran, S., Mawson, R., and Simons, L., *Innov. Food Sci. Emerg. Technol.*, 2008, vol. 9, p. 170.
25. Ghosh, V., Mukherjee, A., and Chandrasekaran, N., *Ultrason. Sonochem.*, 2013, vol. 20, p. 338.
26. Li, M., Ma, Y., and Cui, J., *LWT-Food Sci. Technol.*, 2014, vol. 59, p. 49.
27. Lu, W.-C., Chiang, B.-H., Huang, D.-W., and Li, P.Y., *Ultrason. Sonochem.*, 2014, vol. 21, p. 826.
28. Prabhakar, K., Afzal, S.M., Surender, G., and Kishan, V., *Acta Pharm. Sin.*, vol. 3, p. 345.
29. Li, Y., Zheng, J., Xiao, H., and McClements, D.J., *Food Hydrocolloids*, 2012, vol. 27, p. 517.
30. Kourniatis, L.R., Spinelli, L.S., Piombini, C.R., and Mansur, C.R.E., *Colloid J.*, 2010, vol. 72, p. 396.
31. Solans, C. and Sole, I., *Curr. Opin. Colloid Interface Sci.*, 2012, vol. 17, p. 246.
32. Sole, I., Maestro, A., Pey, C.M., Gonzalez, C., Solans, C., and Gutierrez, J.M., *Colloids Surf. A*, 2006, vol. 288, p. 138.
33. Sole, I., Pey, C.M., Maestro, A., Gonzalez, C., Porras, M., Solans, C., and Gutierrez, J.M., *J. Colloid Interface Sci.*, 2010, vol. 344, p. 417.
34. Anton, N. and Vandamme, T.F., *Int. J. Pharm.*, 2009, vol. 377, p. 142.
35. Pérez, E.P., Alves, D., Enright, M.C., Bean, J.E., Gaudion, A., Jenkins, A.T.A., Young, A.E.R., and Arnot, T.C., *Biotechnol. Prog.*, 2014, vol. 30, p. 932.
36. Izquierdo, P., Feng, J., Esquena, J., Tadros, T.F., Dederen, J.C., Garcia-Celma, M.J., Azemar, N., and Solans, C., *J. Colloid Interface Sci.*, 2005, vol. 285, p. 388.
37. Pey, C.M., Maestro, A., Solé, I., González, C., Solans, C., and Gutierrez, J.M., *Colloids Surf. A*, 2006, vol. 288, p. 144.
38. Sajjadi, S., *Langmuir*, 2006, vol. 22, p. 5597.
39. Sagitani, H., *Surfactant Sci. Ser.*, 1992, vol. 44, p. 259.
40. Forgiarini, A., Esquena, J., Gonzalez, C., and Solans, C., *Langmuir*, 2001, vol. 17, p. 2076.
41. Preziosi, V., Perazzo, A., Caserta, S., Tomaiuolo, G., and Guido, S., *Chem. Eng. Trans.*, 2013, vol. 32, p. 1585.
42. Fernandez, P., Andre, V., Rieger, J., and Kuhnle, A., *Colloids Surf. A*, 2004, vol. 251, p. 53.
43. Shinoda, K. and Saito, H.J., *J. Colloid Interface Sci.*, 1968, vol. 26, p. 70.
44. Shinoda, K. and Saito, H.J., *J. Colloid Interface Sci.*, 1969, vol. 30, p. 258.
45. Izquierdo, P., Esquena, J., Tadros, T.F., Dederen, C., Garcia-Celma, M.J., Azemar, N., and Solans, C., *Langmuir*, 2002, vol. 18, p. 26.
46. Anton, N., Saulnier, P., Beduneau, A., and Benoit, J.-P., *J. Phys. Chem. B*, 2007, vol. 111, p. 3651.
47. Ee, S.L., Duan, X., Liew, J., and Nguyen, Q.D., *Chem. Eng. J.*, 2008, vol. 140, p. 626.
48. Wadle, A., Förster, T., and Rybinski, W.V., *Colloids Surf. A*, 1993, vol. 76, p. 51.

49. Morales, D., Gutierrez, J.M., García-Celma, M.J., and Solans, C., *Langmuir*, 2003, vol. 19, p. 7196.
50. Formiga, F.R., Fonseca, I.A., Souza, K.B., Silva, F.R., Macedo, J.P., Araujo, I.B., Soares, L.A., and Egito, E.S., *Int. J. Pharm.*, 2007, vol. 344, p. 158.
51. Klassen, P.L., George, Z., Warwick, J., and Georgiadou, S., *Colloids Surf. A*, 2014, vol. 455, p. 1.
52. http://www.drugbank.ca/drugs/.
53. Rao, J. and McClements, D.J., *J. Agric. Food Chem.*, 2010, vol. 58, p. 7059.
54. http://www.sigmaaldrich.com/catalog/product/sial/235989?lang=en&region=RU.
55. Schönfeldt, N., *Grenzfachenaktive Athylenoxid-Addukte*, Stuttgart: Wissenschaftliche, 1976.
56. Izquierdo, P., Esquena, J., Tadros, T.F., Dederen, C., Feng, J., Garcia-Celma, M.J., Azemar, N., and Solans, C., *Langmuir*, 2004, vol. 20, p. 6594.
57. Sharif, A.A.M., Astaraki, A.M., Azar, P.A., Khorrami, S.A., and Moradi, S., *Arabian J. Chem.*, 2012, vol. 5, p. 41.
58. Zadymova, N.M., Karmasheva, N.V., Poteshnova, M.V., Tsikurina, N.N., *Colloid J.*, 2002, vol. 64, p. 400.
59. Zadymova, N.M., Tsikurina, N.N., and Poteshnova, M.V., *Colloid J.*, 2003, vol. 65, p. 314.
60. Lehnert, S., Tarabishi, H., and Leuenberger, H., *Colloids Surf. A*, 1994, vol. 91, p. 227.
61. Kantarci, G., Ozguney, I., Karasulu, Y., Arzik, S., and Guneri, T., *AAPS PharmSciTec*, 2007, vol. 8, p. 75.
62. Tavares, L., Shevchuk, I., Alfonso, M., Marcenyak, G., and Valia, K. US Patent 7018649, 2006.
63. Sottman, T. and Strey, R., *J. Chem. Phys.*, 1997, vol. 106, p. 8606.
64. Tadros, T., Izquierdo, P., Esquena, J., and Solans, C., *Adv. Colloid Interface Sci.*, 2004, vols. 108–109, p. 303.
65. Wennerström, H., Balogh, J., and Olsson, B.U., *Colloids Surf. A*, 2006, vol. 291, p. 69.
66. Lifshits, I.M. and Slezov, V.V., *Zh. Eksp. Teor. Fiz.*, 1958, vol. 35, p. 479.
67. Lifshitz, I.M. and Slyozov, V.V., *J. Phys. Chem. Solids*, 1961, vol. 19, p. 35.
68. Wagner, C.Z., *Z. Electrochem.*, 1961, vol. 65, p. 581.
69. Kabal'nov, A.S., Pertsov, A.V., and Shchukin, E.D., *Kolloidn. Zh.*, 1984, vol. 46, p. 1108.
70. Kabalnov, A.S. and Shchukin, E.D., *Adv. Colloid Interface Sci.*, 1992, vol. 38, p. 69.
71. Sakai, T., Kamogawa, K., and Nishiyama, K., *Langmuir*, 2002, vol. 18, p. 1985.
72. *Handbook of Aqueous Solubility Data*, Yalkowsky, S.H. and He, Y., Eds., Boca Raton: CRC, 2003.

Translated by A. Kirilin